Passive Building Walls

Xing Jin

Contents

Abstract

The heat flows through the building envelopes take a large part in the cooling or heating load of a room. Therefore, the thermal performances of building envelopes have a significant influence on the heating or cooling energy consumption in buildings. In this chapter, several passive building walls in building envelopes are introduced, with more attention on phase change material (PCM) walls and green walls. The benefits of PCM walls and the PCM containment in building walls are first summarized, and then the experimental and numerical research studies on the optimal PCM location in the wall are presented. In addition, the energy-saving

X. Jin (✉)
School of Architecture, Southeast University, Nanjing, China
e-mail: jxining@163.com

R. Wang, X. Zhai (eds.), *Handbook of Energy Systems in Green Buildings*,
https://doi.org/10.1007/978-3-662-49120-1_35

potentials of green walls are discussed, and their functions of improving air quality are also analyzed.

Keywords
Passive building · Building walls · Phase change material · Green wall · Energy saving

Introduction

The energy consumption in buildings is a significant issue in a lot of countries. In United States of America, the energy consumption in buildings is more 40% of the total primary energy consumption [1], while in China, the proportion is more than 20%, and it is still increasing. The building energy consumption includes heating, cooling, lighting, cooking, and appliances, etc. While the heating and cooling energy consumptions take up the largest part with more than 50% of total building energy consumption, especially in developed countries.

A building envelope, also known as building enclosure, is what separates the indoor and outdoor environments of a building. It is the key factor that determines the quality and controls the indoor conditions irrespective of transient outdoor conditions [2]. A typical building envelope usually consists of walls, roofs, windows, doors, etc. Both the above-grade and the below-grade portions of the building envelope are part of a physical system involving three interactive components: the exterior environment(s), the envelope system, and the interior environment(s) [3].

The heat flows through the building envelopes takes a large part in the cooling or heating load of a room. Therefore, the building envelopes have a significant influence on the heating or cooling energy consumption in buildings. As such, the use of energy in the building sector can be reduced by improving the thermal performances of their envelopes.

Building walls are the most important components of building envelopes, because they normally have the most areas compared with other components of envelopes. Building walls are expected to provide thermal and acoustic comfort within a building, without compromising the aesthetics of the building [2]. Building walls create a route for thermal transmission due to their large surface area. Conversely they also provide a large surface that facilitates thermal radiation in cold environments. As the high-rise buildings have a high ratio of wall to envelope, the thermal performance of walls can be even more crucial. Appropriate selection of wall type and improving the thermal performance of walls are very effective to reduce the building energy consumption [4].

One of the most important aspects of the green building is its low energy consumption, which is why it is critical to design an effective building energy system. Building energy efficiency can be improved by implementing either active energy efficient strategies like improving the performances of the heating devices, cooling devices, ventilation system, and electrical lighting, or passive strategies like improving the thermal performances of the building envelopes. In the past decades, the

researches about the passive strategies have attracted more and more attentions. It has been proved that a proper architectural design of a building envelope can significantly reduce the energy usage through daylighting, reduced HVAC loads, etc. [2].

The most common passive building walls include phase change material (PCM) walls, green walls, Trombe walls, double skin walls, and autoclaved aerated concrete walls, etc. All of these wall types have been successfully used in buildings and have been proved to have great potentials of energy saving. The objective of this chapter is to introduce these wall types and their corresponding performances.

Phase Change Material Walls

Overview

The most commonly used practice for improving the thermal performance of building envelopes is to increase the total thermal resistance of walls by adding more insulation. In many cases, this may not be practical because of the limitations of wall thickness or for economic reasons. An alternative practice to enhance envelope thermal performance is to increase its thermal storage capacity. This offers improved building envelope heat transfer control, which results in energy use and energy demand reductions, enhanced occupant comfort, and increased equipment operating life [5].

Thermal energy storage is generally classified as sensible and latent heat storage. Different from sensible heat energy storage which stores heat by temperature increase, latent heat storage systems store heat via phase transitions. PCMs are engineered substances that store heat by changing its phase at pre-determined temperature ranges based on application. It is well documented that PCMs provide relatively high heat storage density while requiring smaller masses and volumes of material. For example, the specific capacity of water is 4.2 kJ/(kg K), while its latent heat from water to ice is about 334 kJ/kg. For this reason, building envelopes integrated with PCMs have received increased attention for the purpose of reducing building sector energy use and enhancing occupant thermal comfort [5].

There are three kinds of PCMs based on the phase change state: solid-gas PCMs, solid-liquid PCMs, and liquid-gas PCMs. Generally, the solid-liquid PCMs are the most suitable for thermal energy storage due to its requirement on smaller volumes of material.

Figure 1 shows the classification of the PCMs. The solid-liquid PCMs comprise organic PCMs, inorganic PCMs, and eutectics [6]. A comparison of these different kinds of PCMs is listed in Table 1 [6].

Benefits of PCM Walls

Compared with traditional building envelope, the thermal mass of building envelope integrated with PCMs increases greatly, which could reduce the building energy

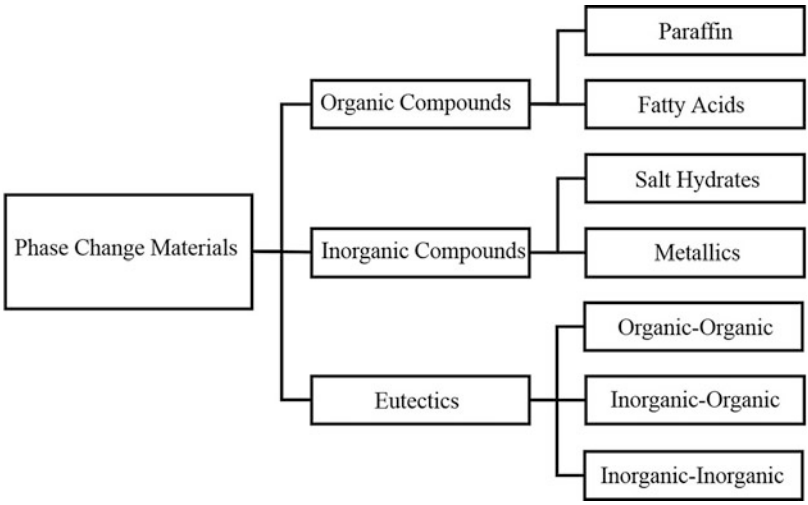

Fig. 1 PCMs classification [6]

Table 1 Comparison of different kinds of PCMs [6]

Classification	Advantages	Disadvantages
Organic PCMs	1. Availability in a large temperature range 2. High heat of fusion 3. No supercooling 4. Chemically stable and recyclable 5. Good compatibility with other materials	1. Low thermal conductivity (around 0.2 W/(m K)) 2. Relative large volume change 3. Flammability
Inorganic PCMs	1. High heat of fusion 2. High thermal conductivity (around 0.5 W/(m K)) 3. Low volume change 4. Availability in low cost	1. Supercooling 2. Corrosion
Eutectics	1. Sharp melting temperature 2. High volumetric thermal storage density	1. Lack of currently available test data of thermo-physical properties

consumption, improve the indoor thermal comfort, and shift the peak electricity load, etc.

Figure 2 shows the experimental data on the wall interior surface heat flux with and without PCM. It is found that the wall with PCM has smaller heat flux fluctuations [7]. Figure 3 shows the numerical results about the interior surface heat fluxes of the walls with and without PCM in 20 days of summer. It is found that the peak heat flux can be reduced greatly [8].

Castell et al. [9] found that the cubicle with PCM wall could reduce energy consumption compared with the same cubicle without PCM. As shown in Table 2,

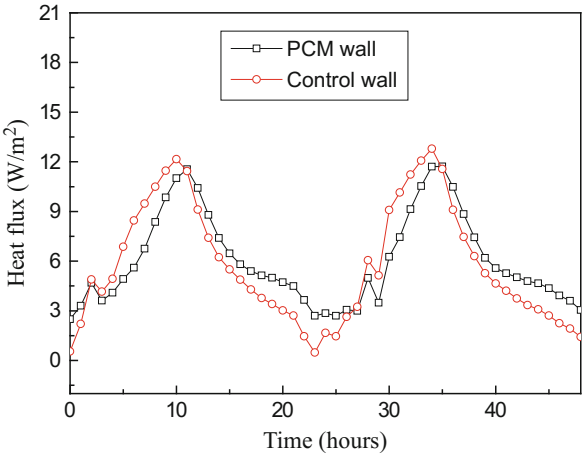

Fig. 2 Experimental heat fluxes of the PCM wall and the control wall [7]

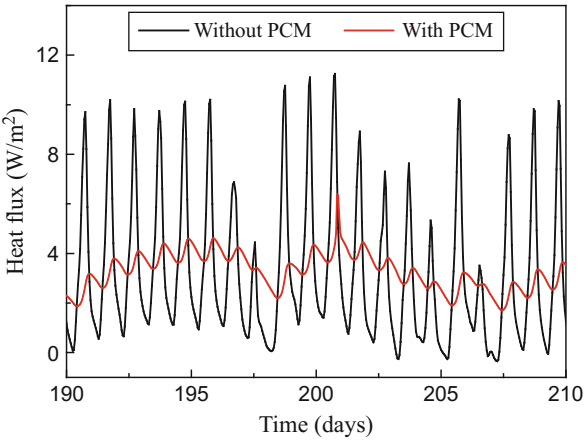

Fig. 3 Numerical results about the interior surface heat fluxes of the walls with and without PCM in summer [8]

the RT27 (a kind of PCM) + PU cubicle achieves a reduction of 15% compared to the PU cubicle, while the SP25 (a kind of PCM) + Alveolar cubicle reaches a 17% of energy savings compared to the Alveolar one. Moreover, the SP25 + Alveolar cubicle presents lower energy consumption than the PU cubicle.

The research conducted by Diaconu et al. [10] also found that the wall with PCM could reduce the energy used for cooling and heating, and the peak load, as shown in Table 3.

PCM Containment in Building Walls

The PCM can change its state from solid to liquid when it absorbs heat. Therefore, the leakage problem must be avoided when the PCM is integrated into building walls. There are several ways to integrate the PCM into building walls: the direct

Table 2 Accumulated energy consumption and savings for the different cubicles [9]

	Energy consumption (Wh)[a]	Energy savings (Wh)[b]	Energy savings (%)[b]	Improvement (%)[c]
Reference	9376	0	0	\
PU	4583	4793	51.12	0
RT27 + PU	3907	5469	58.33	14.75
Alveolar	5053	4323	46.11	0
SP25 + Alveolar	4188	5188	55.33	17.12

[a]Set point of 24 °C during 5 days
[b]Referred to the reference cubicle
[c]Referred to the cubicle with analogue constructive solution and without PCM

Table 3 Maximum values of energy savings and peak load reduction [10]

	Cooling (%)	Heating (%)
Maximum energy savings	1.0	12.8
Maximum reduction of the peak load	24.3	35.4

impregnation in building materials, the macroencapsulation, the microencapsulation, and the shape-stabilized PCM.

The direct impregnation is the simplest method for PCM containment in building walls. The liquid PCM will be absorbed by the building materials such as gypsum, concrete, or other porous materials.

The macroencapsulation means that the PCM will be put in a special container which could be tubes, balls or bags. Then, that container will be integrated into building walls. Figure 4 shows several examples of this method.

The microencapsulation means that the PCM will be put in a microscopic polymer capsule whose diameter is usually shorter than 1000 μm. The microcapsules will form a powder, which then will be included in the recipe of a building construction material. Special attention has to be paid into the choice of the capsule's material in order to avoid chemical reactions between the capsules and the building material. Thus, the PCM will be trapped and cannot leak anymore, and the size of the capsule will be small enough to prevent from a disproportionate isolation of the solid crust of the PCM [11].

More and more researchers have been attracted to the shape-stabilized PCM because it has a good structural property and there is no leakage problem. Shape-stabilized PCM is prepared from a liquid mixture of the PCM and a supporting material. The mixture is then cooled below the glass transition temperature of the supporting material until it becomes solid. An appropriate choice of the supporting material allows PCM mass proportions up to 80%. The most common supporting materials found in the literature are high-density polyethylene (HDPE) and styrene-butadiene-styrene (SBS) [11]. Figure 5 shows the pictures of a kind of shape-stabilized PCM.

The phase change temperature of the PCM used in the wall is usually between 20 °C and 30 °C. Table 4 shows several PCMs which have already been used in the walls [17].

Fig. 4 Macroencapsulation (**a**) [12] (**b**) [13] (c) [14] (**d**) [15]

Optimal PCM Location in the Wall

In previous research, the PCM layer was usually placed close to the indoor environment. For example, a wallboard immersed with PCMs was placed on the interior surface of the wall. Other locations for a PCM layer, such as close to the exterior surface of the wall, or next to the internal face of gypsum board, or within the insulation cavity have appeared in literature. Because PCMs have their own melting temperature ranges and given that temperature profiles across walls differ, PCMs experience different thermal cycles when they are placed in different locations within walls. That is, PCM location in the walls affects phase change process, and it is critical for the optimum thermal performance of walls outfitted with PCMs. As a result, the placement of PCMs within building walls should be evaluated [7].

Experimental Study

Jin et al. [5] studied the effects of the location of a PCM thermal shield (PCMTS) on the thermal performance of the wall by experiments. The thermal performance of the wall with and without PCMTS was tested using a dynamic wall simulator. The three wall panels with PCMTS were referred to as PCM wall A, PCM wall B, and PCM wall C. The last wall panel without PCMTS was referred to as control wall. The

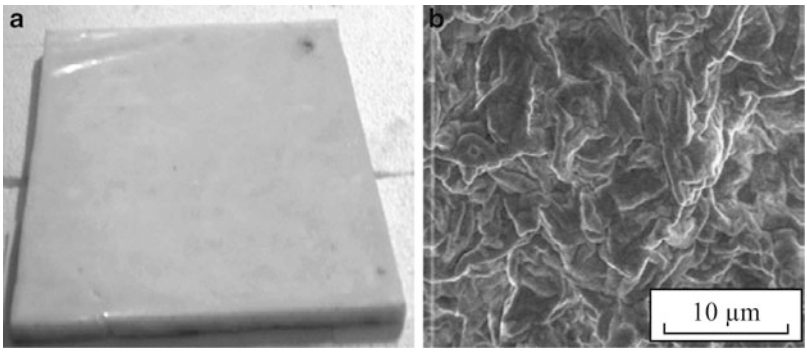

Fig. 5 Shape-stabilized PCM: (**a**) photo of the PCM plate; (**b**) electronic microscopic picture by scanning electric microscope (SEM) [16]

Table 4 PCMs used in the walls [17]

Name of PCM	Category	Phase change temperature (°C)	Heat of fusion (kJ/kg)	Reference
/	Paraffin	20	120	[18]
/	Paraffin	23	115	[19]
RT27	Paraffin	28	179	[20, 21]
TH29	Salt-hydrates	29	175	[20]
CA-PA	Fatty acids	26.2	177	[22]
/	Paraffin	22.2	107	[23]
/	Paraffin	26.2	147.4	[24]
CA-LA	Fatty acids	23	150.3	[25]
/	Salt-hydrates	27	/	[14]
/	Paraffin	24.9	160.3	[26]
RT18	Paraffin	18	134	[15]
MPCM 28-D	Paraffin	28	180–195	[27]
/	Eutectic salts	32	216	[28]
Micronal DS 5001X	Paraffin	26	110	[29]
PEG	Polyethylene glycol	21–25	148	[12]
/	Fatty acids	25.1	181.1	[30]
/	Compounds	28.6	87.3	[30]
/	Paraffin	28.7	100.7	[30]
/	Fatty acids	18.55–26.51	126.4	[31]
/	Paraffin	23.7	131.2	[32]
/	Fatty acids	27, 33, 37, 40	70–85	[33]

structures of the wall with and without the PCMTS are shown in Fig. 6. Because there were five insulating layers in the wall, the entire insulation system was regarded as being dividable into five parts, in which n/5 L, where $0 \leq n \leq 5$, was

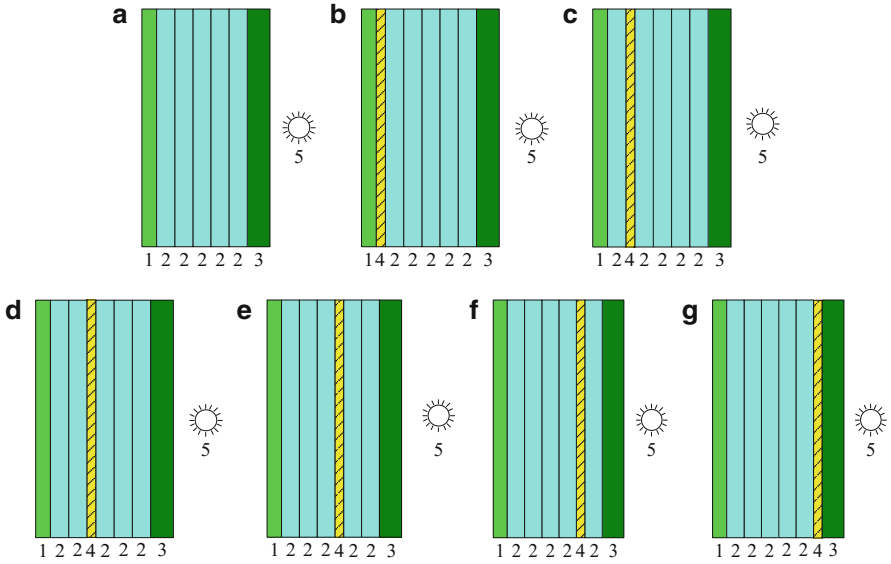

Fig. 6 Schematic of wall construction (**a**) control wall, (**b**) PCM-enhanced wall with PCMTS at location 0/5 L, (**c**) PCM-enhanced wall with PCMTS at location 1/5 L, (**d**) PCM-enhanced wall with PCMTS at location 2/5 L (**e**) PCM-enhanced wall with PCMTS at location 3/5 L, (**f**) PCM-enhanced wall with PCMTS at location 4/5 L, (**g**) PCM-enhanced wall with PCMTS at location 5/5 L. *1*: gypsum wallboard, *2*: insulating layer, *3*: OSB, *4*: PCMTS, *5*: heat source

defined as the distance between any PCM layer in the *n*th location from the internal surface of the gypsum wallboard and L was the thickness of the insulation cavity. That is, when the PCMTS was placed next to the internal surface of the gypsum wallboard, its location was referred to as 0/5 L. Similarly, when the PCMTS was placed between the first and second insulating layers, this location was referred to as 1/5 L, and so on.

Three experiments implemented are aiming to test the thermal performance of the PCMTS in six locations within the walls. In the first experiment, the PCMTSs were installed respectively in the 0/5 L location of PCM wall B, the 1/5 L location of PCM wall A, and the 2/5 L location of PCM wall C. The surface temperatures at either side of the PCMTS for locations 0/5 L, 1/5 L, and 2/5 L are shown in Fig. 7, and in this figure, "warmer" referred to the surface of the PCMTS closer to the heat sources, while "colder" referred to the PCMTS surface closer to the exterior of the simulator. The fact that surface temperatures differed depending on the location of the PCMTS within the wall cavity would lead to different phase change cycles and different effects on the thermal performance of the walls. The heat fluxes across the four walls are shown in Fig. 8. First, it was observed that independent of PCMTS location, the walls that were outfitted with the PCMTS produced lower heat fluxes across the wall, when compared to the control wall. The figure also clearly demonstrates that the

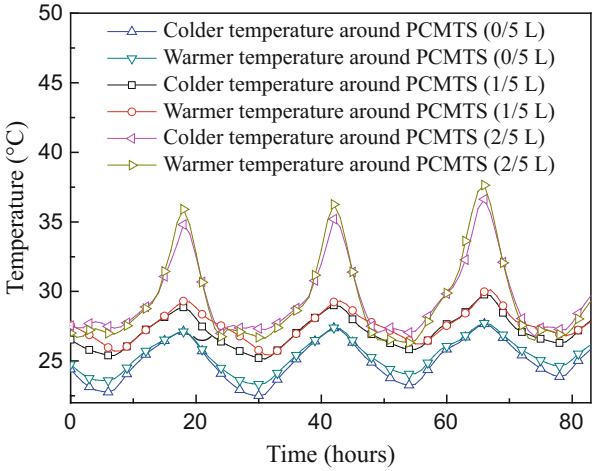

Fig. 7 Temperatures around PCMTS (Experiment 1)

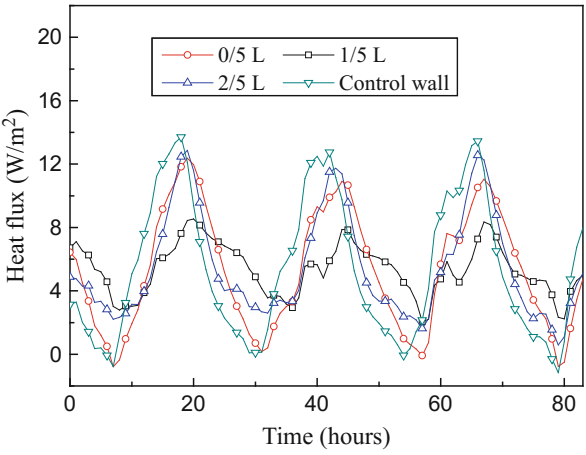

Fig. 8 Heat fluxes across the walls (Experiment 1)

location of the PCMTS had an effect on the reduction of the wall heat fluxes. The data indicated that locating the PCMTS at a distance 1/5 L produced the largest reductions in peak heat fluxes and longest time shift than the other two locations, namely, the 0/5 L and the 2/5 L. In fact, the 0/5 L produced slightly larger reductions than the 2/5 L location. When the PCMTS was located at 1/5 L, the peak heat flux reduction was approximately 38% and the time shift of the peak heat flux was approximately 2 h. Of the three PCMTS locations in this experiment, it was concluded that the 1/5 L was the optimal location.

In the second experiment, the PCMTSs were installed respectively in the 1/5 L location in PCM wall A, the 3/5 L location in PCM wall B, and the 4/5 L location in PCM wall C. The temperature and heat flux variations are shown in Figs. 9 and 10. In regard to the Fig. 10, the highest peak heat flux reduction was also for location 1/5 L.

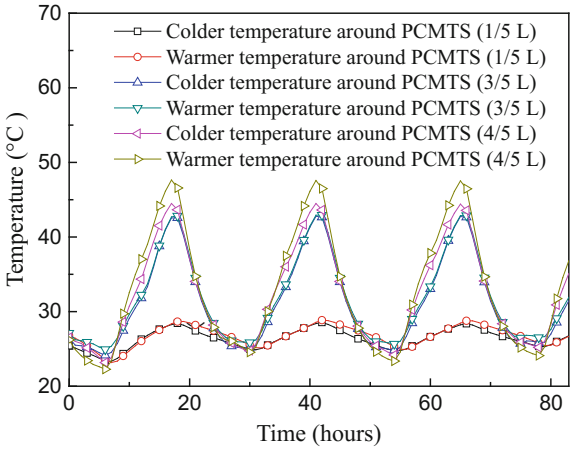

Fig. 9 Temperatures around PCMTS (Experiment 2)

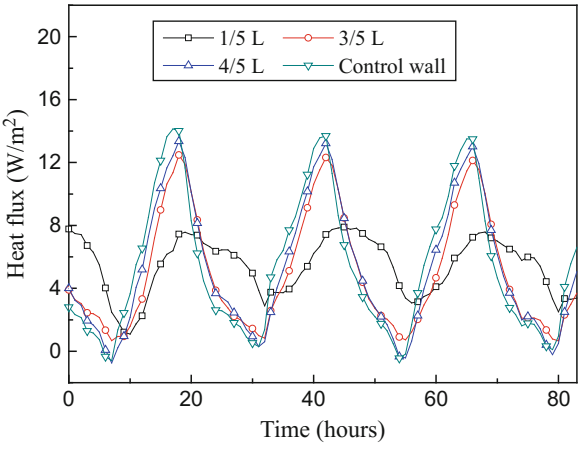

Fig. 10 Heat fluxes across the walls (Experiment 2)

In the third set of experiments, the PCMTSs were installed respectively in the 1/5 L location in PCM wall A and the 5/5 L location in PCM wall C. The temperature and heat flux variations are shown in Figs. 11 and 12. It was also observed from Fig. 12 that location 1/5 L produced the highest heat flux reduction and longer time shift than location 5/5 L. Based on experiments one and two and except for location 1/5 L, the trend was that the closer the PCMTS shield was to the heating source, the less its influence on reducing the peak heat flux and the shorter the peak heat flux time shift.

Because the experimental conditions were not exactly the same during all three experiments, the effects of the PCMTS were a slight different even when the PCMTS was placed in the exact same location. When the PCMTS were placed in the 1/5 L location, the peak heat flux reduction was the highest, with an average of approximately 41%. This location was considered as the optimal place for the location of the PCMTS. In other words, the PCMTS should be installed at a distance of 1/5 L from the internal surface of the bounding wall that is furthest from the heating source. In

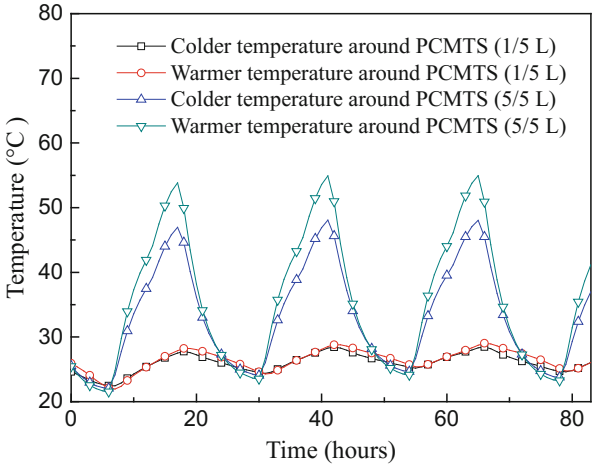

Fig. 11 Temperatures around PCMTS (Experiment 3)

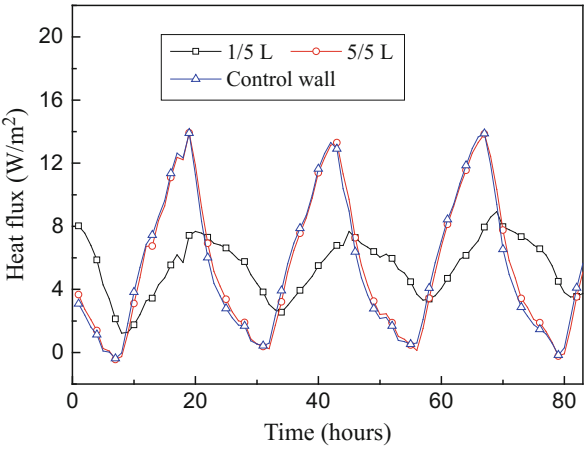

Fig. 12 Heat fluxes across the walls (Experiment 3)

an actual building, this location would be 1/5 L from the internal surface of the wallboard or plasterboard, which is usually in contact with the conditioned space. The second most favorable location was the 0/5 L, or next to the wallboard or plasterboard in contact with the conditioned space. In this location, the peak heat flux reduction produced by the PCMTS was approximately 14%. Figure 13 shows the peak heat flux reductions as a function of PCMTS location.

Numerical Study

In the experimental study, there were six locations for the PCMTS. In the numerical research conducted by Jin et al. [34], the whole insulating layer in the wall was assumed to be divided into 16 parts evenly. Similar with the experimental study above, in which n/16 L, where $0 \leq n \leq 16$, was defined as the distance between any PCM layer in the nth location from the internal surface of the gypsum wallboard and

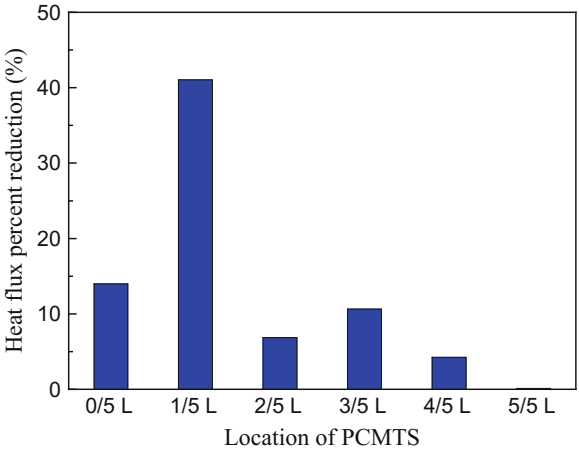

Fig. 13 Heat flux percent reduction as a function of PCMTS location

L was the thickness of the insulation cavity. That is, when the PCM layer was placed next to the internal surface of the gypsum wallboard, its location was referred to as 0/16 L. Similarly, when the distance between the PCM layer and the gypsum wallboard was 1/16 L, the PCM location was referred to as 1/16 L, and so on.

Figure 14 demonstrates the variations of the interior surface heat flux of the wall in 4 days when the thicknesses of PCM layer were 1 mm, 2 mm, 5 mm, and 7 mm, respectively. The interior surface temperature of the wall was 24 °C. There were 17 locations in the wall for PCM layer, so there were 17 heat fluxes lines in the figure. It was observed that the peak heat flux reduction increased as the thickness of PCM layer increased. The optimal locations of PCM layer were 1/16 L, 2/16 L, 3/16 L, and 3/16 L when the thicknesses of PCM layer were 1 mm, 2 mm, 5 mm, and 7 mm, respectively. That meant the optimal PCM location was closer to the exterior surface of wall with the increase of the thickness of the PCM layer. That was because the PCM was more, the absorbed latent heat was more, and the PCM layer with more masses should be closer to the outdoor environment (heat source) in order to absorb more heat.

Compared with the wall without PCM layer, the peak heat flux reductions of PCM wall in optimal PCM location were 9.48%, 35.91%, 53.99%, and 56.11% when the thicknesses of the PCM layer were 1 mm, 2 mm, 5 mm, and 7 mm, respectively. It was also found that the effects were small when the PCM layer was close to the exterior surface of the wall. The reason was that when PCM was too close to the outdoor environment, it was in liquid state during most of the time; thus, it could not solidify and release the heat, and the PCM could not improve the thermal performance of the wall.

Figure 15 shows the effect of PCM melting temperature on the optimal PCM location. The thickness of PCM layer was 5 mm. Referring to the data of these two figures and Fig. 14c, the optimal PCM locations were 0/16 L, 3/16 L, and 5/16 L when the melting temperatures of PCM were 25 °C, 27 °C, and 29 °C, respectively, which demonstrated that when the melting temperature of PCM was higher, the

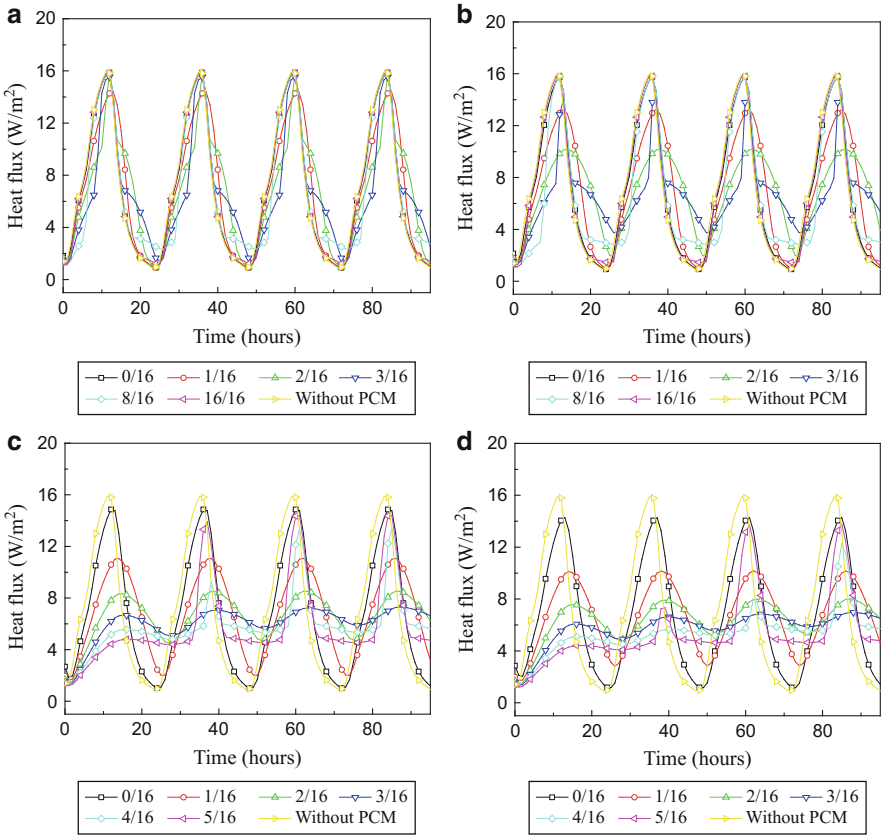

Fig. 14 Effect of the thickness of PCM layer on the optimal PCM location (**a**) 1 mm, (**b**) 2 mm, (**c**) 5 mm, (**d**) 7 mm

optimal location of PCM layer was closer to the exterior surface of the wall. It was because when the melting temperature of PCM was higher, the PCM temperature in the thermal cycles should also be higher for melting. Therefore, the PCM location was closer to the outdoors.

The peak heat flux reductions in the optimal locations were 31.84%, 53.99%, and 53.41% when the melting temperatures of PCM were 25 °C, 27 °C, and 29 °C, respectively. It could be observed that the peak heat flux reductions in optimal locations were almost the same when the PCM melting temperatures were 27 °C and 29 °C, respectively. When the melting temperature of PCM was 25 °C, the peak heat flux reduction in the optimal location was relatively small. It was because when the PCM melting temperature was 25 °C, the optimal location of PCM layer was 0/16 L (next to the gypsum board) which was the innermost location for PCM layer. In fact, if the PCM location was much closer to the interior surface of the wall than location 0/16 L, the peak heat flux reduction would be larger.

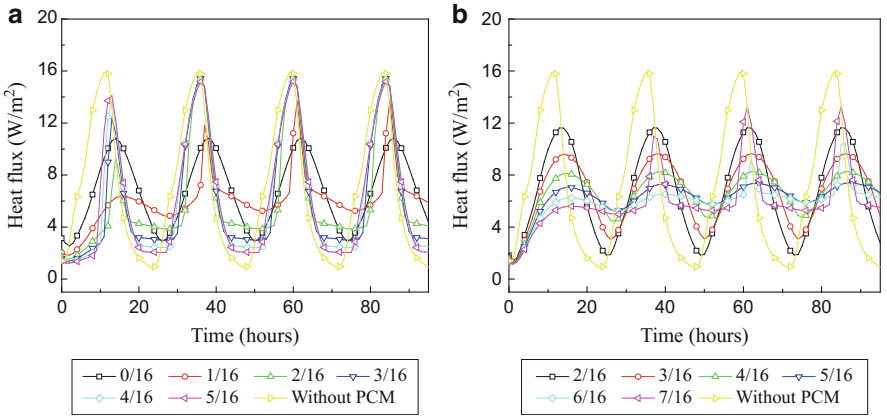

Fig. 15 Effect of the PCM melting temperature on the optimal PCM location (**a**) melting temperature was 25 °C, (**b**) melting temperature was 29 °C

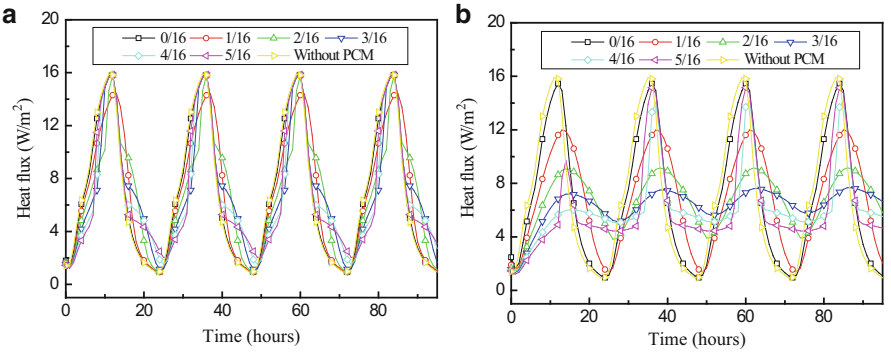

Fig. 16 Effect of the heat of fusion of PCM on the optimal PCM location (**a**) heat of fusion was 80 kJ/kg, (**b**) heat of fusion was 320 kJ/kg

Figure 16 shows the effect of the heat of fusion of PCM on the optimal PCM location. The thickness of PCM layer was 2 mm, the melting temperature of PCM was 27 °C. Referring to these two figures and Fig. 14b, when the heat of fusion was higher, the peak heat flux reduction in the same PCM location was also higher. The optimal locations were 1/16 L, 2/16 L, and 3/16 L when the heat of fusion was 80 kJ/kg, 179 kJ/kg, and 320 kJ/kg, respectively. Base on the data, it could be summarized that when the heat of fusion was larger, the optimal PCM location should be closer to the exterior surface of the wall in order to absorb more heat, while if the heat of fusion was lower, the PCM layer should be closer to the interior surface of the wall to avoid overheating.

Figure 17 shows the effect of interior surface temperature of the wall on the optimal PCM location. The thickness of PCM layer was 5 mm, the melting temperature of PCM was 27 °C, and the heat of fusion of PCM was 179 kJ/kg. Referring to

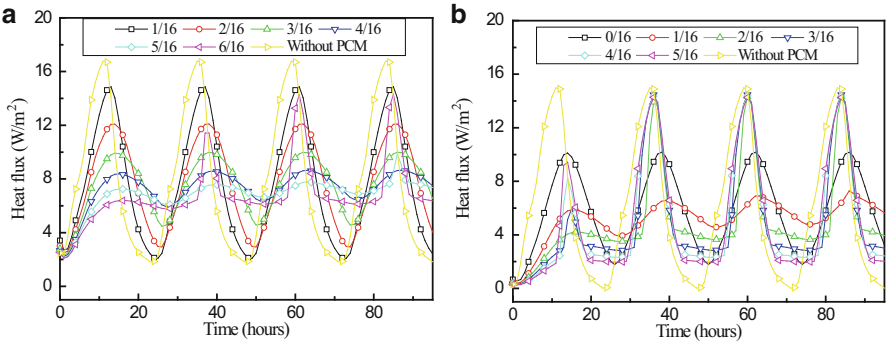

Fig. 17 Effect of the interior surface temperature of the wall on the optimal PCM location (**a**) interior surface temperature was 22 °C, (**b**) interior surface temperature was 26 °C

these two figures and Fig. 14c, the optimal locations were 4/16 L, 3/16 L, and 1/16 L when the interior surface temperatures of the wall were 22 °C, 24 °C, and 26 °C, respectively. It could be summarized that the optimal PCM location was closer to the interior surface of the wall with the increase of interior surface temperature of the wall. It was because when the interior surface temperature of the wall was higher, the PCM temperature in the thermal cycles would also be higher if the PCM location did not change, then PCM would be kept in liquid state and would not be able to release latent heat. Therefore, the optimal location of PCM layer should move to the interior surface of the wall in order to release latent heat when the interior surface temperature of the wall was higher.

Optimal PCM Location Under Nanjing (China) Weather Conditions

The numerical analyses above show that the optimal PCM location in the wall for a typical day could be found. However, this research had its limitations. For example, to simplify the model, the variations of the wall exterior surface temperature in 4 days were the same. It means that the optimal PCM location found out by using the model is optimal only under these conditions in these given 4 days, while it might be not optimal or even be the worst when the outdoor conditions change. In fact, the actual outdoor environment changes day by day, the optimal PCM location in a day may be different from that in other days. For example, the outdoor environments in a sunny day and in a rainy day are totally different, and the optimal PCM location will also be different. When the PCM is used in building walls, the PCM wall should have good thermal performances in a season, especially in summer or in winter, not only in a typical day. In other words, the thermal performances of the PCM walls during a season or a year should be evaluated [8].

Nanjing (32°3′ N, 118°47′ E) is a city in China. It is hot in summer and cold in winter. Table 5 shows the average dry-bulb temperature, the average relative humidity, and the total amount of solar radiation of each month in Nanjing.

The interior surface heat flux fluctuation of the wall could be reduced via the integration with PCM. In other words, it is recognized that the wall with smaller heat

Table 5 Average dry-bulb temperature, average relative humidity and total amount of solar radiation of each month in Nanjing

Month	Average dry-bulb temperature (°C)	Average relative humidity (%)	Total amount of solar radiation (MJ/m^2)
1	2.2	75.5	232.4
2	4.5	76.6	222.0
3	8.9	69.4	387.6
4	15.7	72.8	405.3
5	20.6	70.7	465.6
6	24.8	77.3	480.3
7	28.6	79.8	484.3
8	27.7	81.4	485.0
9	23.5	74.7	381.8
10	16.9	72.5	318.8
11	10.5	78.6	261.3
12	4.9	69.1	229.0

flux fluctuation has better thermal performance. Therefore, the heat flux fluctuation reduction rate is used to evaluate the effects of PCM on the thermal performance of the wall, and it is defined as the following equation.

$$\sigma = \frac{\left(q_{w,\max} - q_{w,\min}\right) - \left(q_{p,\max} - q_{p,\min}\right)}{q_{w,\max} - q_{w,\min}} \tag{1}$$

where σ is the heat flux fluctuation reduction rate. $q_{w,\max}$, $q_{w,\min}$ are the maximum interior surface heat flux and the minimum interior surface heat flux of the wall without PCM during a day. $q_{p,\max}$, $q_{p,\min}$ are the maximum interior surface heat flux and the minimum interior surface heat flux of the wall with PCM during a day.

The larger heat flux fluctuation reduction rate means that the fluctuation of heat flux through the wall is smaller, and the PCM wall has better thermal performance.

The heat flux fluctuation reduction rate during a period time refers to the average heat flux fluctuation reduction rate of all the days in this period.

Just the same as the numerical model above, there are also 17 locations for the PCM layer in the wall.

Table 6 shows the average heat flux fluctuation reduction rates of the PCM wall during different seasons when the PCM layer was placed in different locations. The values in bold demonstrate that the locations were optimal. As shown in the table, the optimal PCM locations in spring, summer, autumn, winter, and a whole year were 8/16 L, 2/16 L, 5/16 L, 8/16 L, and 4/16 L, respectively. When the PCM was placed in the optimal locations in spring, summer, autumn, winter, and a whole year, the average heat flux fluctuation reduction rates were 23.5%, 74.1%, 32.9%, 13.1%, and 33.8%, respectively.

Table 6 demonstrates that even though it was in the same period of four seasons (spring, summer, autumn, winter) or a whole year, the average heat flux fluctuation

Table 6 Heat flux fluctuation reduction rates of PCM wall when PCM layer was placed in different locations during different seasons

PCM locations	Heat flux fluctuation reduction rates (%)				
	Spring	Summer	Autumn	Winter	A year
0/16 L	13.5	64.6	21.7	2.2	25.7
1/16 L	16.0	70.9	26.7	4.8	29.8
2/16 L	18.2	**74.1**	29.3	7.0	32.4
3/16 L	20.0	73.3	31.1	8.9	33.5
4/16 L	21.3	70.3	32.4	10.4	**33.8**
5/16 L	22.3	65.5	**32.9**	11.6	33.2
6/16 L	22.9	61.4	32.7	12.4	32.5
7/16 L	23.3	58.5	32.5	13.0	31.9
8/16 L	**23.5**	55.3	32.3	**13.1**	31.2
9/16 L	23.4	51.7	32.0	13.0	30.1
10/16 L	23.0	47.4	31.4	12.6	28.7
11/16 L	22.3	43.9	30.6	11.8	27.2
12/16 L	21.3	40.6	29.5	10.6	25.6
13/16 L	19.8	36.7	28.1	9.2	23.5
14/16 L	17.6	32.2	25.4	7.3	20.7
15/16 L	13.9	26.3	21.3	5.1	16.7
16/16 L	11.4	18.5	14.6	2.5	11.8

reduction rates were different when the PCM was placed in different locations because it experienced different thermal cycles even under the same outdoor/indoor environments.

Besides, the average heat flux fluctuation reduction rates in different seasons were different even with the same PCM location. Take location 2/16 L as an example, it was the optimal PCM location in summer but obviously not in other seasons. Especially in winter, the average heat flux fluctuation reduction rate was only 7% in this location. That was because for most of the time in winter, the PCM temperature was lower than its phase change temperature, which meant it was not able to melt. Accordingly, the PCM did not have much effect on the heat flux fluctuation reduction.

Figure 18a shows the interior surface heat fluxes of the wall when the PCM was placed in different locations in 20 days of summer. Figure 18b shows the PCM temperatures variations in these 20 days. As shown in Fig. 18a, when the PCM location was 2/16 L, the fluctuation of wall heat flux was the smallest. This could be proved by its temperature variations in Fig. 18b, it was found that the PCM temperature was in its phase change temperature range almost in the whole period, which meant that the phase change process of the PCM was always performed. Therefore, the wall had the best thermal performance in this location. While when the PCM locations were 8/16 L and 16/16 L, as shown in Fig. 18b, the PCM temperature was higher than 28 °C and it was in the liquid state for most of the time due to the very high outdoor temperature in summer. It was obvious to observe that the effects of the PCM in these locations were smaller than those in location 2/16 L.

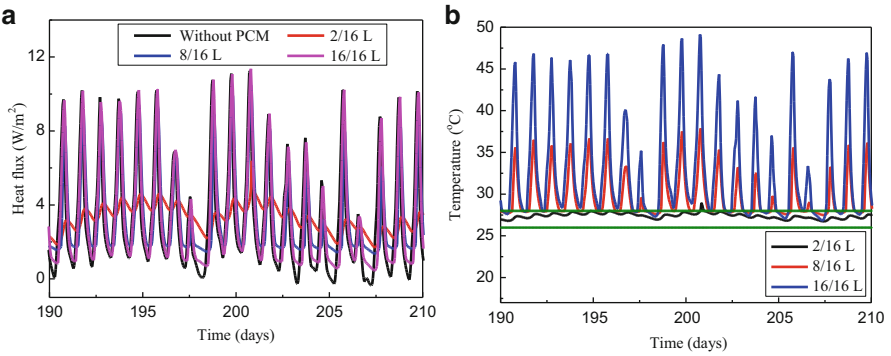

Fig. 18 Variations of wall heat fluxes and PCM temperatures in 20 days of summer (**a**) wall heat fluxes; (**b**) PCM temperatures

Table 7 Heat flux fluctuation reduction rates with different phase change temperature ranges in summer

PCM location	Heat flux fluctuation reduction rate/%						
	18–20 °C	20–22 °C	22–24 °C	24–26 °C	26–28 °C	28–30 °C	30–32 °C
0/16 L	1.7	1.7	1.7	19.8	64.6	2.7	1.7
1/16 L	3.7	3.7	3.7	24.2	70.9	16.1	3.7
2/16 L	5.6	5.6	5.6	27.1	**74.1**	25.5	6.8
3/16 L	7.3	7.3	7.3	29.4	73.3	37.8	13.5
4/16 L	8.7	8.7	8.9	31.1	70.3	47.3	19.9
5/16 L	9.8	9.8	10.3	32.3	65.5	54.6	24.4
6/16 L	10.6	10.6	11.7	33.1	61.4	59.8	29.8
7/16 L	11.1	11.1	13.3	33.7	58.5	**64.3**	36.0
8/16 L	**11.3**	**11.3**	14.7	**33.8**	55.3	64.2	41.6
9/16 L	11.2	11.3	15.9	33.7	51.7	63.8	45.7
10/16 L	10.7	10.9	16.8	33.2	47.4	61.8	49.6
11/16 L	10.0	10.4	**17.4**	32.3	43.9	58.6	51.3
12/16 L	8.9	9.4	17.4	30.7	40.6	54.5	**51.4**
13/16 L	7.5	8.4	16.8	28.8	36.7	50.3	49.9
14/16 L	5.9	7.1	15.6	26.2	32.2	44.9	46.4
15/16 L	4.1	5.7	13.8	21.8	26.3	36.1	38.8
16/16 L	2.1	4.0	11.0	16.2	18.5	24.9	26.7

Table 7 shows the heat flux fluctuation reduction rates with different phase change temperature ranges and different PCM locations in summer. Because the outdoor temperature was very high in this season, when the PCM phase change temperature was lower than 26 °C (the indoor air temperature), it was in liquid state and not able to release the latent heat for most of the time, and the heat flux fluctuation reduction rates were small. When the phase change temperature was higher than 26 °C, the optimal PCM location was closer to the outdoor environment with the increase of the

phase change temperature. That was because the PCM should be closer to the heat source to melt when its phase change temperature was high. It was also found that the optimal PCM phase change temperature range was 26–28 °C, and the optimal PCM location was 2/16 L in this range.

Green Walls

Overview

The unstoppable force of urbanization is consuming vast quantities of natural vegetation that is replaced by concrete buildings and surfaces with low albedos. These resulting changes in the thermal properties of surface materials and the lack of evapotranspiration in urban areas lead to a phenomenon known as the urban heat island effect. With the idea of bringing nature back into the urban landscape, a partnership between nature and the city is being strengthened aiming to create a new sustainable urban lifestyle. Greenery is the key element of this transformation. Since the outer surfaces of building offer a great amount of space for vegetation in urban cities, planting on roofs and walls has become one of the most innovative and rapidly developing fields in the worlds of ecology, horticulture, and the built environment [35].

Green walls, which are also known as vertical greenery systems (VGSs) or green vertical systems, mean that the growing of plants directly or indirectly (with special constructions) on the side of the building facade. Green walls have been a traditional architectural feature since ancient times. Climbing plants have been used in building facades since the seventeenth century in the UK, Europe, and North American cities [36].

In the research conducted by Pérez et al. [37], green walls can be subdivided into two main systems: green facades and living walls. Green facades are facade systems in which climbing plants or hanging port shrubs are developed by using special support structures, mainly in a directed way, to cover the desired area. The plants can be planted directly in the ground at the base of the structure, or in pots at different heights of the facade. Living walls are made of panels and/or geotextile felts, sometimes precultivate, which are fixed to a vertical support or on the wall structure. The panels and geotextile felts provide support to the vegetation formed by upholstering plants, ferns, small shrubs, and perennial flower, among others [37].

As green walls could bring the nature vegetation without occupying any ground space, it has been recognized as an effective way to improve the urban environment. Four pictures of the green walls are shown in Fig. 19.

Now, green walls have been more and more popular in cities because of their environmental and ecological benefits. At a city scale, green roofs and green walls contribute to the insertion of vegetation in the urban context without occupying any space at street level. In fact, covering buildings with vegetation, when applied in a significant urban scale, can improve the urban environment by contributing to the increase of urban biodiversity, the management of storm water, the improvement of

Fig. 19 Examples of green walls (**a**) Lleida, Spain [37]; (**b**) Golegã, Portugal [38]; (**c**) Hong Kong, China; (**d**) Nanjing, China

air quality, the reduction of temperature, and the mitigation of heat island effect. At the same time, the application of greening systems could offer social and economic benefits beside the environmental advantages. These systems encourage the fruition of urban areas, have a therapeutic effect by inducing a psychological wellbeing through the presence of vegetation, improve cities image, increase property value, and function as a complementary thermal and acoustic protection [38]. At a building scale, green wall systems can be used as a passive design solution contributing to buildings sustainability performance. Vegetation has potentials to improve the microclimate both in winter by functioning as a complementary insulation layer and in summer by providing shade and an evaporative cooling effect. Vegetation absorbs large amounts of solar radiation while the effect of evapotranspiration of plants can further reduce the impact of solar radiation, which indicates increasing humidity levels and surface temperatures are lower than hard surfaces. Recent studies show that green wall systems have the ability to control heat gains and losses, contributing to improve indoor thermal comfort and reduce energy demands for heating or cooling [38].

Energy Saving Potential of Green Walls

Like wearing a coat, green walls reduce the heat transfer between outdoors and indoors. In addition, green walls in summer could also be used as shading devices, which could reduce indoor solar heat gain. In this way, the cooling load and the building electricity consumption in summer could be reduced.

Pan and Chu [39] quantified the environmental benefits of a commercially available vertical greenery system. The electricity consumptions for cooling in flats with and without a vertical greenery system (8.22 m^2) in a public housing estate in Hong Kong were compared and presented below.

The experimental site was located in a 33-storey Housing Authority estate under construction in Sheung Shui, New Territories, Hong Kong. Two identical flats (Fig. 20) were selected: a flat on the 4th floor with vertical greenery installed on the external wall and a flat on the 5th floor without wall greenery, which was the control.

Figure 21 shows the half-hourly temperature fluctuations for the exterior concrete surfaces of the bare and experimental walls. A positive ΔT value indicated a higher exterior concrete surface temperature of the bare wall than that of the vegetated wall. The temperature difference reached 1–8 °C during sunny days and a maximum of approximately 5 °C on cloudy days. Figure 22 shows the regression between the daily average temperature and the electricity saving associated with vertical greenery system. It was found that the electricity saving of the two flats was correlated to the ambient conditions. There was a significant correlation ($P < 0.001$) between the daily average temperature and the electricity saving in summer. The results showed that the electricity saving associated with green wall increased with the average daily temperature.

Table 8 shows the air-conditioning electricity consumption of the two flats with and without a vertical greenery system. The daily electricity consumption of the flat

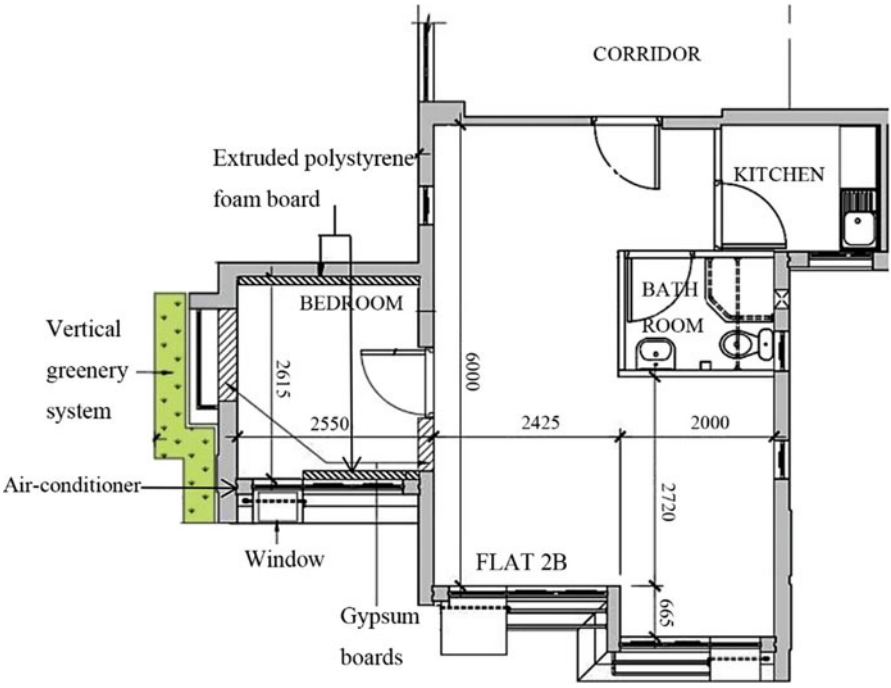

Fig. 20 Layout plan of the experimental flats [39]

without vertical greening was higher than that of the flat with vertical greening in both August and September. The daily electricity saving by the vertical greenery system in sunny, cloudy and rainy day in summer were 1.30, 0.84, and 0.71 kWh, respectively. Under all weather conditions, the flat with vertical greenery system had lower cooling load than the control flat due to the reduction of heat transfer. The best cooling effect occurred on sunny days, followed by cloudy and rainy days. The average daily electricity saving attributable to the vertical greenery system was estimated to be 16%.

According to the pattern of local energy use, air-conditioning accounts for 17% of all the energy consumption. The total energy consumption in Hong Kong in August and September was 17362 and 15619 TJ, respectively. Based on the data of energy saving obtained in this study, the potential for energy saving from vertical greening would be 472 and 425 TJ for the 2 months, respectively. These figures indicated significant energy savings in the urban environment, although the actual amount saved would be affected by factors like climate, system design, and energy use for air-conditioning. Based on the tariff and fuel cost ($0.805 and $0.270 per kWh in the study area), and estimated total electricity saving by the vertical greenery system in 1 year, the monetary value of electricity saving by a vertical greenery system would be HK$144 (US$1.00 = HK$7.75). The economic cost of energy consumption could be reduced due to the cooling effect of the vertical greenery systems on

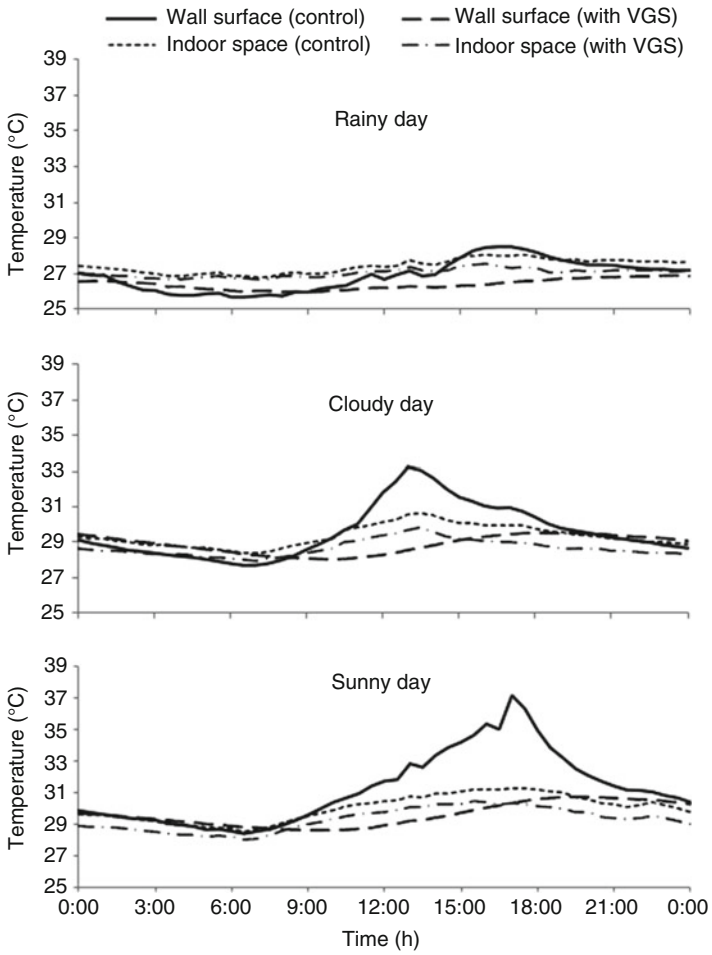

Fig. 21 Half-hourly temperature change over a day in flats with and without vertical greening under different weather conditions (sunny, cloudy, and rainy days) during August and September 2013 [39]

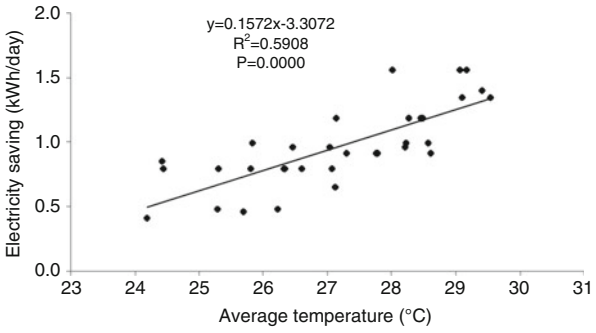

Fig. 22 Regression between the daily average temperature and the electricity saving associated with vertical greening during August and September 2013 [39]

Table 8 Air-conditioning electricity consumption at whole-day operation mode on three summer sample days at the two flat with and without a VGS in August and September 2013 [39]

Season-weather	Sampled days (number)	Daily energy consumption (kWh)		Daily energy saving by VGS (kWh)	Daily energy saving by VGS (%)	Total days from June to September (number)	Estimated energy saving by VGS from June to September (kWh)
		Without VGS	With VGS				
Summer-sunny	17	7.12	5.82	1.30	18.3	62	80.6
Summer-cloudy	11	5.97	5.13	0.84	14.0	28	23.4
Summer-rainy	7	5.24	4.52	0.71	13.6	42	30.0
Summer-total	35	18.3	15.5	2.85	15.8	132	134

building envelopes, and the initial investment on the vertical greenery systems could be paid back in roughly 40 years.

Coma et al. [40] compared the thermal performance of two different vertical greenery systems implemented in experimental houses-like cubicles for both cooling and heating periods. The experimental site was located in Puigverd de Lleida, Catalonia, a north-east area in Spain at latitude 41°N under Mediterranean continental climatic conditions.

Those three house-like cubicles with identical walls and roofs construction systems have been built for the implementation of the experiments. Their external dimensions are 3 × 3 × 3 m and can be considered as real scale experiments but under controlled conditions as in laboratories. Compared with the reference cubicle, the cubicles with green walls had plants on their walls.

Because Boston ivy is ease to climb and it presents well adaptation to the specific climatic conditions of the experimental site, so it was selected for the green wall A. Two different evergreen shrubs (*Rosmarinus officinalis* and *Helichrysum thianschanicum*) were selected for the green wall B due to its well adaptation to survive in a Mediterranean climate. It was noted that in their paper, green wall A was referred to as double-skin green facade and green wall B was referred to as green wall. These three cubicles are shown in Fig. 23.

Table 9 summarizes the electrical energy consumption of the heat pumps of each cubicle, the set point temperature, the duration of the tests, as well as the energy savings of the vertical greenery system cubicles.

Regarding the energy consumption, the green wall B had the big potential energy savings up to 58.9% during cooling periods as demonstrated through the performed experiments compared with the reference during the studied period of July under controlled temperature at 24 °C inside the cubicle. Moreover, the green wall A also showed significant energy savings up to 33.8% for the same period. However, depending on the indoor set point temperature, a nonlinear cooling performance

Fig. 23 Studied cubicles in the experimental set-up (**a**) Reference; (**b**) green wall A; (**c**) green wall B [40]

Table 9 Total cumulative electrical energy consumption of the heat pumps during cooling experimental period of the three studied cubicles [40]

Period	Set-point (°C)	Number of analyzed days	Accumulated energy consumption (kWh)			Average energy savings (%)	
			Green wall A	Green wall B	Reference	Green wall A	Green wall B
June 2015	18	10	33.99	24.63	35.78	5.01	31.16
June 2015	21	11	16.72	11.98	20.98	20.32	42.93
July 2015	24	12	21.01	13.04	31.75	33.83	58.94

could be observed. This is because the contribution of the vertical greenery system is directly related to the solar irradiance as well as the cooling required by the demand.

The hourly energy consumed by each cubicle and the solar irradiance of two consecutive summer days are shown in Fig. 24. On one hand, compared to greenery

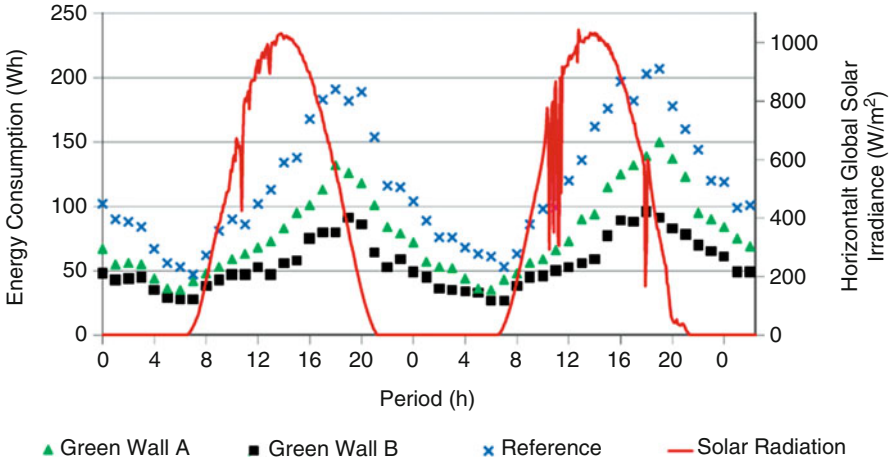

Fig. 24 Hourly electrical energy consumption (6 and 7 July 2015).Controlled temperature at 24 °C (cooling) [40]

systems, the expected higher energy consumption of the reference cubicle was clearly reflected, reaching more than double values during peak hours (from 18:00 to 20:00). In addition, the delay between the solar irradiation peak (which occurs from 13:00 to 14:00) and the electrical energy consumption peak was about 5 h for all cubicles, which was directly related to the high thermal inertia of the wall construction system based on alveolar bricks.

On the other hand, after sunset (21:00), the energy consumption of all cubicles tended to be similar for the next 7 h due to the absence of solar irradiance and, consequently, with no effect of the shadow from the green wall. Nevertheless, the heat pump of the reference cubicle still consumed more energy during nights (00:00–04:00) to remove the heat stored in walls during daytime while trying to achieve the established internal set point. The lowest differences in energy consumption among the three cubicles were from 04:00 to 08:00.

The energy performance versus the daily average vertical solar irradiation of both green wall A and green wall B is shown in Fig. 25. For 12 consecutive days' testing under the set point temperature at 24 °C, compared with the energy consumed by the reference system, the green wall B showed higher energy savings, ranging from 50.9% to 75.4%, while the green wall A showed values between 26% and 47.2%. In regard to the data, the green wall B reduced the energy consumption 23.4% every 1000 Wh/m^2 of incident daily vertical solar irradiation, while the green wall A provided a reduction of 19.4%. On the other hand, the energy performance of both green walls versus the outside air temperature had been analyzed, showing no correlation between them and demonstrating that the solar irradiance was the key parameter to determine whether the green wall could be effectively used as passive system.

Table 10 summarizes all parameters and results obtained in heating experiments: the electrical energy consumption of the heat pumps of each cubicle, the set point

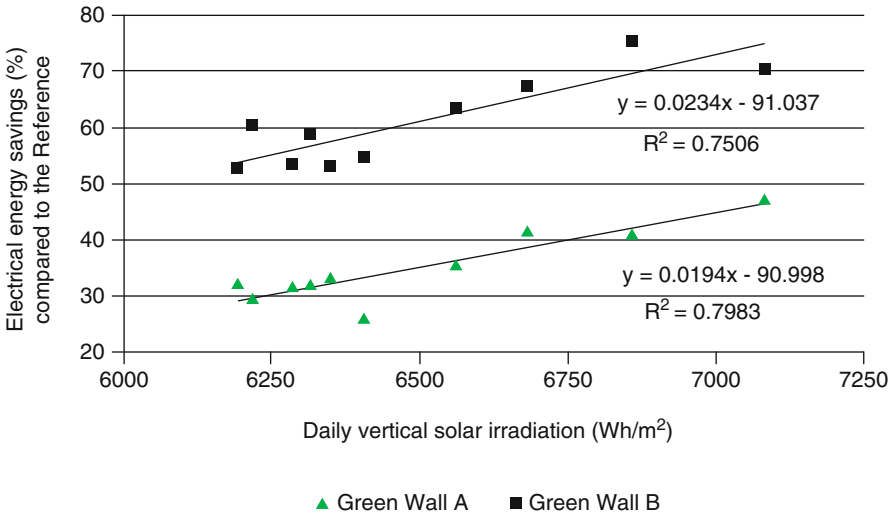

Fig. 25 Thermal performance of green walls versus the daily average vertical solar irradiation received by each cubicle during 12 days testing with a set point of 24 °C [40]

Table 10 Total cumulative electrical consumption of the heat pumps during heating experimental period of the three studied cubicles [40]

Period	Set-point (°C)	Number of analyzed days	Accumulated energy consumption (kWh)			Average energy savings (%)	
			Green wall A	Green wall B	Reference	Green wall A	Green wall B
Dec 2014	22	17	93.00	89.92	92.66	−0.36	2.96
Jan–Feb 2015	22	9	53.69	52.43	54.73	1.90	4.20

temperature, the duration of the tests, and the energy performance of the green wall cubicles in comparison to the reference one.

As shown in the table, the green wall A, covered by deciduous creepers plants (Boston ivy), took advantage of solar gains during the heating period and allowed solar radiation to reach the building facade walls. This effect implied that there was no extra electrical energy consumption during winter period in the cubicle with green wall A for the studied period.

On the other hand, the cubicle with green wall B, covered by evergreen and opaque, demonstrated an interesting slight reduction of energy demand during the heating period. That fact could be attributed to their night radiative protection (insulation effect) supplied by vertical polyethylene modules filled with substrate. The external surface walls of the green wall B radiated less energy to the sky, while the green wall A and Reference cubicles had a direct wall exposure to the sky.

According to the obtained results, no major differences among the three cubicles in their behaviors were found during the heating period. Therefore, it could be concluded that the incorporation of the vertical greenery system on the facades of a building by means of green walls would not penalize the thermal behavior of this building during winter periods.

Even in the case of the green wall B, and given the addition of a new layer on the building envelope, an extra insulation effect was provided to the building, which could be improved in the future with new and better module designs (thickness, type of substrate, type of plants, irrigation regime, etc.).

Air Quality Improvement Potential of Green Walls

Street-level concentrations of nitrogen dioxide (NO_2) and particulate matter (PM) exceed public health standards in many cities, causing increased mortality and morbidity [41]. As an initiative of introducing urban greening concepts to reduce the impacts of harmful pollutants in the atmosphere, green infrastructure practices such as trees, shrubs, lawns, green roofs, and green walls have been widely used in various urban areas across the world and have been proved to be efficient to reduce the harmful air pollutants and regulating the greenhouse gas emissions within the cities. The vegetation intercepts gaseous air pollutants through the leaf stomata as the primary way of improving air quality. Furthermore, the vegetation can intercept particulate matter by absorbance or adherence to the surface with the aid of the wind currents [42].

Green walls offer a way to control the air pollution by enhancing deposition velocities to in-canyon surfaces. Pugh et al. [41] studied the effectiveness of green infrastructure for improvement of air quality in urban street canyons.

Figure 26 shows the in-canyon concentration reduction by using green walls. The green walls across large areas of street canyons could reduce the concentrations of NO_2 and PM_{10} by as much as 15% and 23% when the wind speed is 1 m/s and aspect ratio (i.e., height/width; h/w) is 1. These reductions were strongly dependent on residence time and fraction of canyon wall greening but not on the initial pollutant concentration. As cities are a major regional source of air pollutants, for cities with large areal coverage of street canyons, this is expected to make an important difference to pollutant transport and regional scale photochemistry.

Jayasooriya et al. [42] analyzed the air quality improvement through several green infrastructure scenarios consisting of trees, green roofs, and green walls based on a case study area in Melbourne, Australia, whose picture is shown in Fig. 27.

For the green walls scenario, vertical walls of plantation were added to the industrial and commercial buildings (boundaries of the buildings), just as shown in Fig. 28. Hedges of 2 m high *Laurus nobilis* species were added to commercial buildings as green walls.

Figure 29 shows the annual air pollutant removal for the green wall scenario in comparison with the base-line scenario with no green walls in all the buildings for

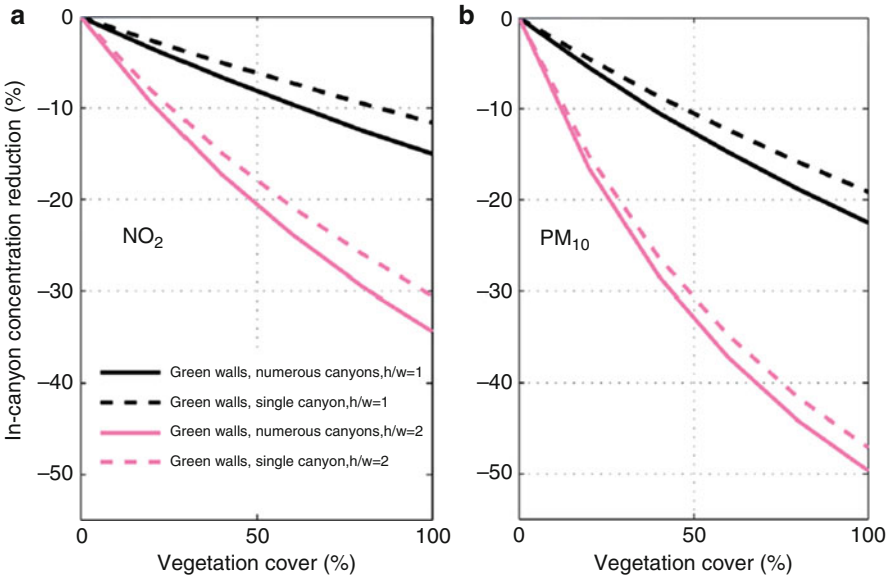

Fig. 26 In-canyon concentration reduction (relative to no vegetation cover) in daytime (06:00–18:00) as a function of wall vegetation coverage (**a**) NO_2; (**b**) PM_{10} [41]

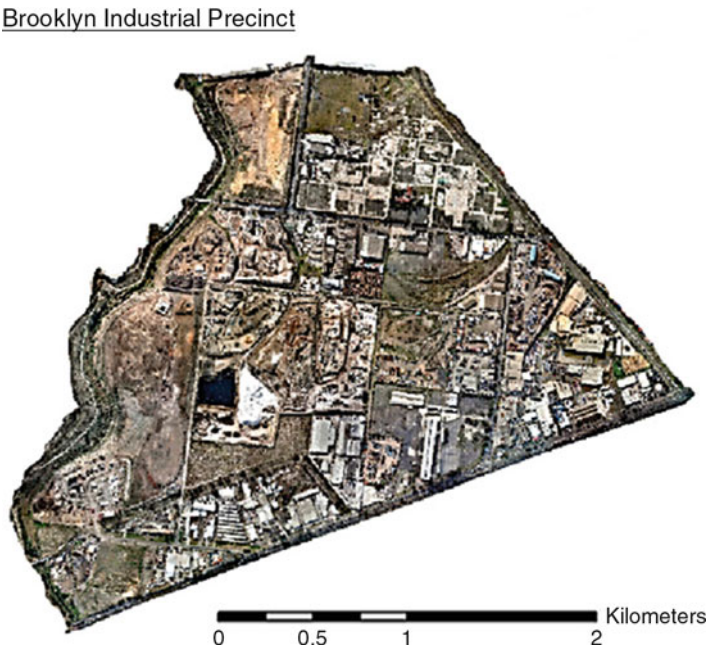

Fig. 27 Plot selection of study area [42]

Fig. 28 Green wall scenario [42]

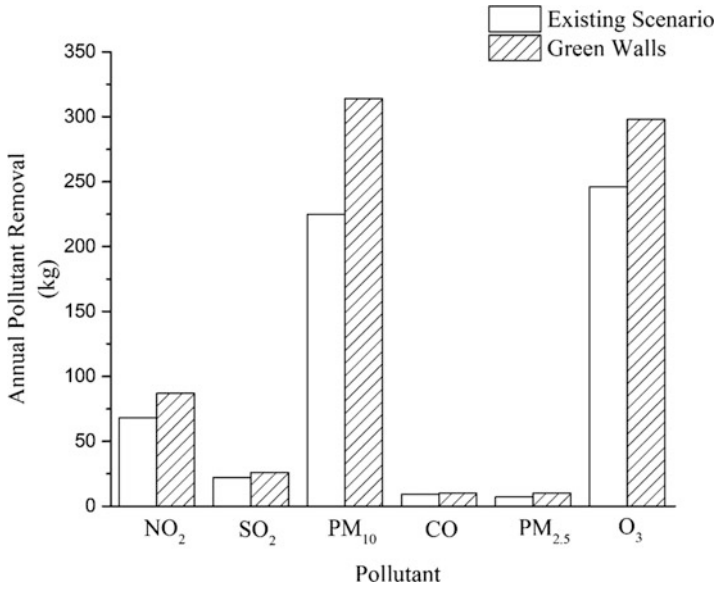

Fig. 29 Annual air pollutant removal for the green wall scenario in comparison with the existing scenario [42]

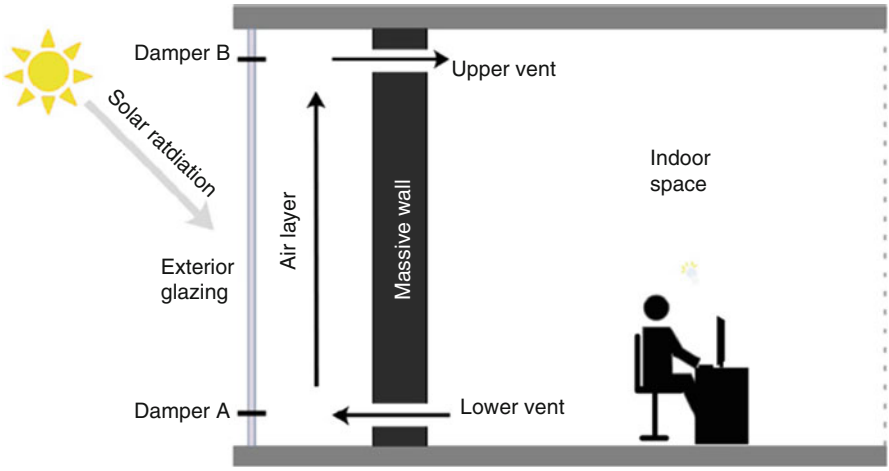

Fig. 30 Schematic diagram of classical Trombe wall [44]

the study area. Replacing the building walls by green walls improved the air quality annually by up taking 87 kg of NO_2, 26 kg of SO_2, 314 kg of PM_{10}, 10 kg of CO, 10 kg of $PM_{2.5}$, and 298 kg of O_3. Therefore, it could be concluded that the green walls had a great potential to improve the urban air quality.

Other Passive Building Walls

Trombe Walls

The concept of Trombe wall was first explored by E.S. Morse in the nineteenth century and developed and popularized in 1957 by Félix Trombe and Jacques Michel. In 1967, in Odeillo, France, they built the first house using a Trombe wall [43]. As shown in Fig. 30, the Trombe wall mainly consists of a massive wall, an exterior glazing cover, and an air channel between the massive wall and the cover. The massive wall is used for absorbing and storing the solar energy that passes through the glazing cover. It must be constructed with high heat-storage capacity materials, such as bricks, concrete, stone, and adobe, and the external surface of the massive wall is usually colored black in order to increase the solar absorption [44].

The classic Trombe wall can catch solar radiation exploiting greenhouse effect produced in a glazed cavity by absorbing and storing heat through its massive wall. Part of the energy is transferred into the indoor of building or the room through the wall by conduction. Meanwhile, the lower temperature air enters the cavity from the room through the lower vent of the wall, heated up by the wall and flows upward due to buoyancy effect. The heated air then returns to the room through the upper vent of the wall [43]. Therefore, the Trombe wall could provide free heating to the room

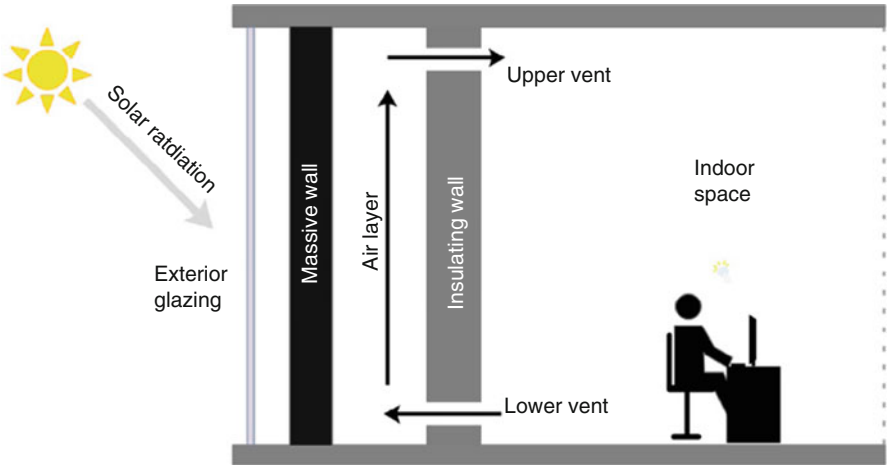

Fig. 31 Schematic diagram of composite Trombe-Michel wall [44]

without any mechanical devices and the heating energy consumption of the building would be reduced consequently.

To increase the thermal resistance of the classic Trombe wall and control supplies, another heating-based type of Trombe wall, which is known as composite Trombe wall or Trombe–Michel wall, is developed [43]. As shown in Fig. 31, the structure of the composite Trombe wall is similar to that of the classical Trombe wall except that an insulating wall is located at the back of the massive wall. Thus, a typical Trombe-Michel wall consists of several layers, including an exterior glazing cover, an enclosed air cavity, a massive wall, a ventilated air channel, and an insulating wall. The absorbed heat can be transferred to the moving air layer by conduction and convection through the massive wall. Then the circulating air takes the thermal energy to the indoor space. In nighttime and nonsunny daytime of winter, the air vents in the insulating wall should be closed to prevent heat loss from inside to outside of the room [44].

Double Skin Facades

Double skin facades, also known as double skin walls, were firstly proposed in early 1900s, but it had been progressed little until the 1990s. The double skin facades are now becoming a popular architectural element on the premise that more and more transparent facades are employed in modern office buildings, and building energy efficiency becomes a critical point of global energy utilization [44].

Double skin facade is defined as a special type of exterior building envelope, which is composed of an external facade layer, an interior facade layer, and an air layer in between. The external layer, usually a hardened single layer of float glass or safety glass, provides protection against the outdoor condition and extra acoustic

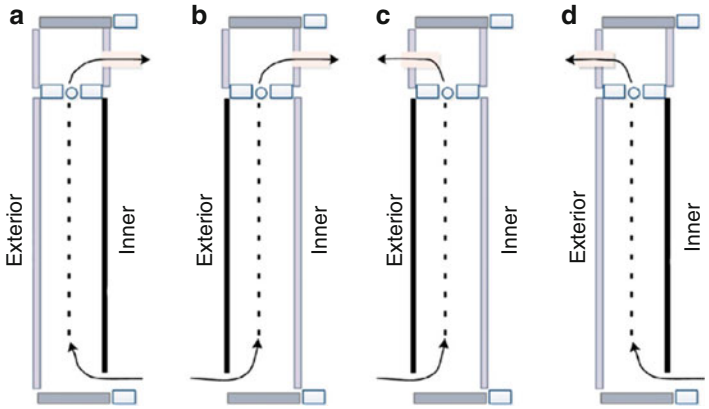

Fig. 32 Schematic of the working modes of double-skin facade: *A* – inner circulation mode; *B* – supply mode; *C* – inner circulation mode; *D* – exhaust mode [44]

insulation against external noise, while the interior layer often consists of double-pane glasses. The width of the air space between the two skins, named the air channel, ranges from 200 mm to more than 2 m. Usually, an adjustable sun shading system is installed in the air channel for controlling solar radiation. The double skin facades can work either in an air-fixed mode that provides extra thermal insulation for external envelopes to reduce heat transfer in winter, or an air-ventilated mode that deals with overheating problems in summer and helps to achieve energy savings in winter. The working modes of double skin facades are shown in Fig. 32 [44].

With proper design, the benefits of the double skin facades include very good daylighting, excellent view, attractive esthetic values, better nature ventilation, and lower energy consumption.

Conclusion

The use of energy in the building sector can be reduced by improving the thermal performance of their envelopes. Nowadays, passive building walls have attracted more and more attentions and have been used a lot in modern residential and commercial buildings because of their great energy-saving potentials and other social and economic benefits.

In this chapter, the most common passive building walls including PCM walls, green walls, Trombe walls, and double skin walls are introduced, with more attention on PCM walls and green walls.

Compared with traditional building walls, the thermal mass of PCM walls increases greatly, which could reduce the building energy consumption, improve the indoor thermal comfort, and shift the peak electricity load. The benefits of

PCM walls and the PCM containment in building walls are summarized, and the experimental and numerical research studies on the optimal PCM location in the wall are also presented. As green walls could bring the nature vegetation to the city without occupying any ground space, they are recognized as an effective way to improve the urban environment. The energy-saving potentials of the green walls are discussed. In addition, their functions of air quality improvement are also analyzed.

References

1. https://www.eia.gov/consumption/
2. Sadineni SB, Madala S, Boehm RF (2011) Passive building energy savings: a review of building envelope components. Renew Sustain Energy Rev 15:3617–3631
3. Straube J, Burnett E (2005) Building science for building enclosures. Building Science Press, Westford
4. Omrany H, Ghaffarianhoseini A, Ghaffarianhoseini A, Raahemifar K, Tookey J (2016) Application of passive wall systems for improving the energy efficiency in buildings: a comprehensive review. Renew Sustain Energy Rev 62:1252–1269
5. Jin X, Medina MA, Zhang XS (2013) On the importance of the location of PCMs in building walls for enhanced thermal performance. Appl Energy 106(06):72–78
6. Zhou D, Zhao CY, Tian Y (2012) Review on thermal energy storage with phase change materials (PCMs) in building applications. Appl Energy 92:593–605
7. Jin X, Medina MA, Zhang XS (2014) On the placement of a phase change material thermal shield within the cavity of buildings walls for heat transfer rate reduction. Energy 73(8):780–786
8. Jin X, Shi DS, Medina MA, Shi X, Zhou X, Zhang XS (2017) Optimal location of PCM layer in building walls under Nanjing (China) weather conditions. J Therm Anal Calorim 129:1767–1778
9. Castell A, Martorell I, Medrano M et al (2010) Experimental study of using PCM in brick constructive solutions for passive cooling. Energy Build 42:534–540
10. Diaconu BM, Cruceru M (2010) Novel concept of composite phase change material wall system for year-round thermal energy savings. Energy Build 42:1759–1772
11. Kuznik F, David D, Johannes K, Roux J-J (2011) A review on phase change materials integrated in building walls. Renew Sustain Energy Rev 15:379–391
12. Ahmad M, Bontemps A, Sallée H et al (2006) Thermal testing and numerical simulation of a prototype cell using light wallboards coupling vacuum isolation panels and phase change material. Energy Build 38(6):673–681
13. Bontemps A, Ahmad M, Johannès K et al (2011) Experimental and modelling study of twin cells with latent heat storage walls. Energy Build 43(9):2456–2461
14. Zalewski L, Joulin A, Lassue S et al (2012) Experimental study of small-scale solar wall integrating phase change material. Sol Energy 86(1):208–219
15. Silva T, Vicente R, Soares N et al (2012) Experimental testing and numerical modelling of masonry wall solution with PCM incorporation: a passive construction solution. Energy Build 49(2):235–245
16. Zhou G, Zhang Y, Zhang Q et al (2007) Performance of a hybrid heating system with thermal storage using shape-stabilized phase-change material plates. Appl Energy 84(10):1068–1077
17. Zhang XS, Xia Y, Jin X (2015) Review on phase change material building walls. J South Univ (Nat Sci) 2015(45):612–618

18. Lin K (2006) Study of the application principles and effects for PCM building envelope components. PhD dissertation, Tsinghua University
19. Kosny J, Kossecka E, Brzezinski A et al (2012) Dynamic thermal performance analysis of fiber insulations containing bio-based phase change materials (PCMs). Energy Build 52(3):122–131
20. Evers AC, Medina MA, Fang Y (2010) Evaluation of the thermal performance of frame walls enhanced with paraffin and hydrated salt phase change materials using a dynamic wall simulator. Build Environ 45(8):1762–1768
21. Borreguero AM, Carmona M, Valverde JL et al (2010) Improvement of the thermal behaviour of gypsum blocks by the incorporation of microcapsules containing PCMS obtained by suspension polymerization with an optimal core/coating mass ratio. Appl Therm Eng 30(10):1164–1169
22. Sayyar M, Weerasiri RR, Soroushian P et al (2014) Experimental and numerical study of shape-stable phase-change nanocomposite toward energy-efficient building constructions. Energy Build 75(2):249–255
23. Kuznik F, Virgone J (2009) Experimental assessment of a phase change material for wall building use. Appl Energy 86(10):2038–2046
24. Shi X, Memon SA et al (2014) Experimental assessment of position of macro encapsulated phase change material in concrete walls on indoor temperatures and humidity levels. Energy Build 71(3):80–87
25. Lv SL, Feng GH, Zhu N et al (2007) Experimental study and evaluation of latent heat storage in phase change materials wallboards. Energy Build 39(10):1088–1091
26. Yan QY, Huo R, Li LS (2012) Experimental study on the thermal properties of the phase change material wall formed by different methods. Sol Energy 86(10):3099–3102
27. Lai C, Chen RH, Lin CY (2010) Heat transfer and thermal storage behaviour of gypsum boards incorporating micro-encapsulated PCM. Energy Build 42(8):1259–1266
28. Carbonari A, De Grassi M, Di Perna C et al (2006) Numerical and experimental analyses of PCM containing sandwich panels for prefabricated walls. Energy Build 38(5):472–483
29. Oliver A (2012) Thermal characterization of gypsum boards with PCM included: thermal energy storage in buildings through latent heat. Energy Build 48(5):1–7
30. Yan QY, Huo R, Zhang L (2011) Experimental research on the heat transfer and mechanical property of shape-stabilized phase change material walls. Build Energy Effic 39(9):42–46
31. Feng GH, Han SY, Liu X et al (2013) Experimental study on night ventilation effect in a phase change wall room in summer. J Shenyang Jianzhu Univ (Nat Sci) 29(4):693–697
32. Chen C, Guo HF, Zhou W (2009) Experimental research of the composite phase change material in greenhouse. Acta Simul Syst Sin 30(3):287–293
33. Deng AZ, Li SB, Zhuang CL et al (2009) Experimental study of heat insulation and energy performance of lightweight PCM building envelope. J Heat Vent Air Cond 39(9):75–79
34. Jin X, Medina MA, Zhang XS (2016) Numerical analysis for the optimal location of a thin PCM layer in frame walls. Appl Therm Eng 103:1057–1063
35. Wong NH, Tan AYK, Chen Y, Sekar K, Tan PY, Chan D, Chiang K, Wong NC (2010) Thermal evaluation of vertical greenery systems for building walls. Build Environ 45:663–672
36. Dahanayake KWDKC, Chow CL (2017) Studying the potential of energy saving through vertical greenerysystems: using EnergyPlus simulation program. Energy Build 138:47–59
37. Pérez G, Rincón L, Vila A, González JM, Cabeza LF (2011) Green vertical systems for buildings as passive systems for energy savings. Appl Energy 88:4854–4859
38. Manso M, Castro-Gomes J (2015) Green wall systems: a review of their characteristics. Renew Sust Energ Rev 41:863–871
39. Pan L, Chu LM (2016) Energy saving potential and life cycle environmental impacts of a vertical greenery system in Hong Kong: a case study. Build Environ 96:293–300
40. Coma J, Perez G, Gracia DA, Bures S, Urrestarazu M, Cabeza LF (2017) Vertical greenery systems for energy savings in buildings: a comparative study between green walls and green facades. Build Environ 111:228–237

41. Pugh TAM, MacKenzie AR, Whyatt JD, Nicholas Hewitt C (2012) Effectiveness of green infrastructure for improvement of air quality in urban street canyons. Environ Sci Technol 46:7692–7699
42. Jayasooriya VM, Ng AWM, Muthukumaran S, Perera BJC (2017) Green infrastructure practices for improvement of urban air quality. Urban For Urban Green 21:34–47
43. Hu ZT, He W, Ji J, Zhang SY (2017) A review on the application of Trombe wall system in buildings. Renew Sustain Energy Rev 70:976–987
44. Zhang TT, Tan YF, Yang HX, Zhang XD (2016) The application of air layers in building envelopes: a review. Appl Energy 165:707–734